Purification and Functional Reconstitution of the Rat Organic Cation Transporter OCT1†

Thorsten Keller,‡ Marco Elfeber,‡ Valentin Gorboulev,‡ Helmut Reiländer,§,|| and Hermann Koepsell*,‡

Institute of Anatomy and Cell Biology, University of Würzburg, Koellikerstrasse 6, 97070 Würzburg, Germany, and Max Planck Institute of Biophysics, Marie-Curie Strasse 15, 60439 Frankfurt am Main, Germany

Received April 13, 2005; Revised Manuscript Received July 18, 2005

ABSTRACT: The rat organic cation transporter rOCT1 with six histidine residues added to the C-terminus was expressed in Sf9 insect cells, and expression of organic cation transport was demonstrated. To purify rOCT1 protein, Sf9 cells were lysed with 1% (w/v) CHAPS [3-[(3-cholamidopropyl)dimethylammonio]-1-propanesulfonate], centrifuged, and subjected to sequential affinity chromatography using lentil−lectin Sepharose and nickel(II)-charged nitrilotriacetic acid−agarose. This procedure yielded ∼70 μg of purified rOCT1 protein from 10 standard culture plates. Using a freeze−thaw procedure, purified rOCT1 was reconstituted into proteoliposomes formed from phosphatidylcholine, phosphatidylserine, and cholesterol. Proteoliposomes exhibited uptake of [^{3}H]-1-Methyl-4-phenylpyridinium ([^{3}H]MPP) that was inhibited by quinine and stimulated by an inside-negative membrane potential. MPP uptake was saturable with an apparent K_m of 30 ± 17 μM. MPP uptake (0.1 μM) was inhibited by tetraethylammonium, tetrabutylammonium, and tetrapentylammonium with IC_{50} values of 197 ± 11, 19 ± 1, and 1.8 ± 0.03 μM, respectively. With membrane potential clamped to 0 mV using valinomycin in the presence of 100 mM potassium on both sides of the membrane, uptake of 0.1 μM MPP was *trans* stimulated 3-fold by 2.5 mM intracellular choline, and efflux of 0.1 μM MPP was *trans* stimulated 4-fold by 9.5 mM extracellular choline. The data show that rOCT1 is capable and sufficient to mediate transport of organic cations. The observed *trans* stimulation under voltage-clamp conditions shows that rOCT1 operates as a transporter rather than a channel. Purification and reconstitution of functional active rOCT1 protein is an important step toward the biophysical characterization and crystallization.

The *SLC22* transporter family comprises polyspecific transporters with a pivotal role in the absorption, excretion, and tissue distribution of drugs and endogenous compounds such as choline, carnitine, and monoamine neurotransmitters (*1*−*3*). To understand the physiological role of these transporters, their tissue distribution, subcellular localization, regulation, substrate specificity, and transport mechanism must be known. A mechanistic understanding of how they operate will help to design drugs that are distributed by these transporters or modulate their function. The rat organic cation transporter rOCT1 was the first cloned member of the *SLC22* family (*4*). rOCT1, its human orthologue hOCT1, and the two other subtypes, OCT2 and OCT3 from rat and human, have been characterized in detail after expression in oocytes of *Xenopus laevis* and in cultured mammalian cells (*4*−*11*). Because OCT1−3 translocate net electric charge, they can be studied using electricophysiological approaches, in addition to isotope uptake assays. Previous studies in intact oocytes and in giant patches from oocytes expressing rat OCT2 indicated that the OCTs facilitate diffusion of organic cations in both directions across the plasma membrane (*5*, *7*, *8*). Moreover, it was shown that the OCTs contain binding regions with partially overlapping binding sites for different substrates that are accessible from both sides of the plasma membrane (*12*). Mutagenesis experiments identified several amino acids in rOCT1 that are critical for affinity and selectivity of substrates and inhibitors (*13*−*15*). The 3D structure of rOCT1 was modeled by homology to the 3D structure of lactose permease from *Escherichia coli* that was determined by X-ray crystallography (*15*). In this model, the amino acids involved in substrate binding were localized within one region of a large cleft that is formed by various transmembrane α-helices. In the present work we were able to express rOCT1 in insect cells, to purify and reconstitute the transporter in artificial liposomes, and to measure rOCT1-mediated uptake of organic cations. Our data provide direct evidence that rOCT1 is sufficient to mediate voltage-dependent organic cation uptake. *Trans* stimulation experiments performed under voltage-clamp conditions strongly suggest that rOCT1 is a typical transporter rather than a channel.

MATERIALS AND METHODS

Materials. [^{3}H]-1-Methyl-4-phenylpyridinium ([^{3}H]MPP,[1] 3.1 TBq/mmol) was obtained from Biotrend (Köln, Germany), 3-[(3-cholamidopropyl)dimethylammonio]-1-propanesulfonate (CHAPS) from AppliChem (Darmstadt, Germany), nickel(II)-charged nitrilotriacetic acid−agarose (Ni^{2+}-

† This work was supported by Deutsche Forschungsgemeinschaft Grant SFB 487/A4.

* Corresponding author. Phone: ++49-(0)931 312700. Fax: ++49-(0)931 312087. E-mail: Hermann@Koepsell.de.

‡ University of Würzburg.

§ Max Planck Insititute of Biophysics.

|| H.R. passed away on February 2, 2005.

10.1021/bi050676c CCC: $30.25
Published on Web 08/19/2005

NTA-agarose) from QIAGEN (Hilden, Germany), lentil−lectin Sepharose from Amersham Biosciences Europe (Freiburg, Germany), *N*-glycosidase F (PNGase F) from Roche Diagnostics GmbH (Penzberg, Germany), protease inhibitors from Calbiochem (Bad Soden, Germany), and polyvinylidene difluoride membranes from Millipore (Eschborn, Germany). Tetrapentylammonium (TPeA) hydroxide, tetrabutylammonium (TBuA) hydroxide, tetraethylammonium (TEA) hydroxide, phosphatidylcholine (PC), phosphatidylserine (PS), cholesterol, lithium hydroxide, cesium hydroxide, and valinomycin were purchased from Sigma-Aldrich (Taufkirchen, Germany). All other materials were obtained as described (*9*, *16*).

DNA Constructs for Expression of rOCT1 in Sf9 Cells. The coding region of rOCT1 was previously cloned into the vector pET22b(+) (Novagen, Madison, WI). rOCT1 was excised with restriction endonucleases *Msc*I and *Bam*HI and ligated to the baculovirus transfer vector pAc360MycHis (*17*) that was digested with *Eco*RI, filled in using the Klenow fragment of *E. coli* DNA polymerase, and cut with *Bam*HI. The resulting vector (pAc360Myc-rOCT1-His) contained rOCT1 with an N-terminal myc epitope and a C-terminal His tag. Sf9 insect cells were cotransfected with the pAc360Myc-rOCT1-His DNA and with linearized baculovirus DNA (BaculoGold; BD Pharmingen, San Diego, CA). Selection of plaques for recombinant virus was performed according to the manufacturer's recommendations. The presence of the rOCT1 coding sequence in the recombinant virus was confirmed by Southern blot analysis. Recombinant virus was grown to a titer of $(4-6) \times 10^7$ pfu/mL and used to transfect insect cells for rOCT1 expression.

Culturing, Transfection, and Harvesting of Sf9 Cells. Sf9 cells were cultured at 27 °C in Grace's insect medium containing 10% (v/v) fetal calf serum and 50 mg/L gentamicin. A suspension of 2×10^8 Sf9 cells (Invitrogen, Karlsruhe, Germany) was transfected with recombinant baculovirus [MOI = 1 (*18*)] and incubated at 27 °C in 75 cm^2 flasks. After 3, 4, or 5 days the cells were harvested by scraping them off the surface of the flasks and collected by 10 min centrifugation at 300*g*. The cells were washed twice by suspension in 25 mL of 1.9 mM NaH_2PO_4, 8.1 mM Na_2HPO_4, and 154 mM NaCl, pH 7.4 (PBS), followed by centrifugation at 300*g*, and suspended in PBS containing 1 mM $CaCl_2$ and 0.5 mM $MgCl_2$ (Ca-PBS).

Transport Measurements in Sf9 Cells. Uptake of [^{3}H]MPP was measured by incubating suspended cells at 30 °C for the indicated time intervals with various concentrations of MPP in Ca-PBS in the absence and presence of 75 μM cyanine863, an inhibitor of the rOCT1 (*4*, *9*). For measurements in the presence of cyanine863, cells were preincubated for 5 min at 30 °C with the inhibitor. Uptake was stopped with 9 volumes of ice-cold PBS containing 100 μM quinine, another inhibitor of rOCT1 (*4*, *9*). Cells were spun down by centrifugation at 8000*g*, washed two times with 100 volumes of ice-cold PBS containing 100 μM quinine, and solubilized by shaking overnight at room temperature in the presence of 4 M guanidine thiocyanate. Scintillation coctail was added, and samples were counted on a Beckman Coulter LS 6500 liquid scintillation counter. MPP uptake after 0 s incubation was measured by adding first ice-cold stop solution to cells and then PBS with [^{3}H]MPP. The protein concentration was determined according to Bradford using bovine serum albumin as a standard (*19*).

Preparation of Membrane Fractions and Deglycosylation. Pelleted Sf9 cells were disrupted by hypotonic lysis in a 10-fold volume of ice-cold H_2O and homogenized by repeated aspiration through a 27-gauge needle. After addition of 2 volumes of ice-cold hypotonic EDTA buffer [5 mM Tris-HCl, pH 7.4, 2 mM EDTA$(Na)_2$] containing protease inhibitors [1 mM 4-(2-aminoethyl)benzenesulfonyl fluoride hydrochloride, 0.8 μM aprotinin, 50 μM bestatin, 15 μM *N*-(*trans*-epoxysuccinyl)-L-leucine-4-guanidinobutylamide, 20 μM leupeptin, and 10 μM pepstatin A] the suspension was centrifuged at 5000*g* and at 4 °C for 30 min. The supernatant was removed, and a crude membrane fraction was isolated as a pellet after 60 min centrifugation at 45000*g* (4 °C). Enriched plasma membranes were isolated by fractionation of crude membranes on a step gradient with sucrose (*20*). For enzymatic deglycosylation, 5 μL of crude membranes or enriched plasma membranes containing 10 μg of protein was pretreated for 10 min at 94 °C with 0.2% (w/v) SDS and then incubated with PNGase F for 18 h at 37 °C [2 units in 20 μL of 30 mM Na_3PO_4, pH 7.5, 20 mM EDTA, 1% (v/v) Triton X-100, and the above indicated cocktail of protease inhibitors]. Controls were treated similarly but without PNGase F.

SDS−Polyacrylamide Gel Electrophoresis (SDS−PAGE) and Western Blotting. For SDS−PAGE, protein samples were pretreated for 30 min at 37 °C in 60 mM Tris-HCl, pH 6.8, 100 mM dithiothreitol, 2% (w/v) SDS, and 7% (v/v) glycerol and then separated by SDS−PAGE as described (*16*). Separated proteins were transferred by electroblotting to a polyvinylidene difluoride membrane and stained for rOCT1 protein as described earlier (*21*) using an affinity-purified polyclonal antibody raised against the large extracellular loop of rOCT1. Bound peroxidase-conjugated secondary antibody (goat anti-rabbit IgG) was visualized by enhanced chemiluminescence (ECL system; Amersham Biosciences Europe, Freiburg, Germany). Prestained molecular weight markers (BenchMark; Life Technologies, Karlsruhe, Germany) were used to determine apparent molecular masses.

Lysis of Sf9 Cells with Detergent and Purification of rOCT1. For lysis, cells from ten 14.5 cm diameter culture plates were suspended in 20 mL of lysis buffer [20 mM Tris-HCl, pH 7.9, 500 mM NaCl, 100 mM choline chloride, 1% (w/v) CHAPS] containing the protease inhibitors described above and shaken for 1 h. Lysis and the subsequent steps of purification were carried out at 4 °C. Insoluble material was spun down by centrifugation for 1 h at 100000*g*. The supernatant was mixed with 2 mL of lentil−lectin Sepharose beads suspended in lysis buffer with protease inhibitors and incubated for 2 h. The suspension was filled into an empty column and the resin washed with 20 mL of lysis buffer. Bound proteins were eluted with 20 mL of lysis buffer containing 300 mM methyl α-D-mannopyranoside. Imidazole was added to the eluate to a final concentration of 5 mM.

[1] Abbreviations: [^{3}H]MPP, [^{3}H]-1-methyl-4-phenylpyridinium; CHAPS, 3-[(3-cholamidopropyl)dimethylammonio]-1-propanesulfonate; Ni^{2+}-NTA−agarose, nickel(II)-charged nitrilotriacetic acid−agarose; PNGaseF, *N*-glycosidase F; HEK, human embryonic kidney; TPeA, tetrapentylammonium; TBuA, tetrabutylammonium; TEA, tetraethylammonium; SDS−PAGE, sodium dodecyl sulfate−polyacrylamide gel electrophoresis; PBS, phosphate-buffered saline.

The mixture was incubated for 2 h with 1 mL of Ni^{2+}-NTA−agarose. After the suspension was filled into a column, the resin was washed with 2 × 5 mL of lysis buffer containing 5 mM imidazole and 20 mM imidazole, respectively. Bound proteins were eluted by 50 mM imidazole in 5 mL of lysis buffer. Fractions (300 μL) were collected and either stored at 4 °C or snap-frozen in liquid nitrogen and stored at −80 °C.

Reconstitution of Purified rOCT1 in Artificial Liposomes. Reconstitution was performed by a previously described freeze−thaw procedure for small amounts of proteins (*22*). *Protein−lipid aggregates* consisting of purified rOCT1 protein plus added lipids were formed by detergent removal and mixed with *multilamellar liposomes* that had been formed by shaking of dried lipids with buffer. This mixture was frozen and thawed. Generation of *transporting proteoliposomes* was promoted by diluting, pelleting, resuspending, and homogenizing of the thawed sample.

To form *protein−lipid aggregates*, we dissolved 1 mg of cholesterol, 1 mg of phosphatidylcholine, and 1 mg of phosphatidylserine in 1 mL of a chloroform/methanol mixture (1/1 v/v) and dried this solution at room temperature under a stream of nitrogen in a 25 mL round-bottom flask. We then added 70 μg of purified rOCT1 protein in 600 μL elution buffer and shook the mixture for 1 h at 4 °C. Subsequently, the detergent was removed by dialysis against 200 mL of 20 mM Tris-HCl, pH 7.9, 500 mM NaCl, and 100 mM choline chloride for 12 h at 4 °C. The obtained suspension was centrifuged for 30 min at 200000*g* (4 °C) and the sediment resuspended in 2 mL of ice-cold KC buffer (100 mM potassium cyclamate, 20 mM imidazole, pH 7.4, 0.1 mM magnesium cyclamate). After another 30 min centrifugation at 200000*g*, the protein−lipid aggregates were suspended in 150 μL of KC buffer and stored at 4 °C.

To prepare *multilamellar liposomes*, 4 mg of phosphatidylserine and 2 mg of cholesterol were dissolved in 1 mL of chloroform/methanol (1/1 v/v) and dried under a stream of nitrogen in a rotating 50 mL round-bottom flask. KC buffer (1 mL) and some glass beads were added, and the flask was shaken for 3 h at room temperature under nitrogen. Aggregates were pelleted by 10 min centrifugation at 10000*g* (room temperature), and multilamellar liposomes in the supernatant were concentrated by centrifugation at 200000*g* for 15 min and resuspension of the pellet in 150 μL of KC buffer (room temperature).

To form *transporting proteoliposomes*, 150 μL of the protein−lipid aggregates was mixed with 150 μL of the multilamellar liposomes and incubated for 15 min at 41 °C. This mixture was snap-frozen in liquid nitrogen. Shortly before transport measurements were started, the sample was thawed by 5 min incubation at 37 °C in a water bath. After addition of 1.7 mL of KC buffer (room temperature) the proteoliposomes were spun down by centrifugation at 200000*g* for 15 min (room temperature). The pellet was suspended in 300 μL of KC buffer (room temperature), and formation of monolamellar proteoliposomes was induced by repeated suction of the suspension into and forced extrusion out of a 100 μL pipet tip.

For control measurements liposomes were formed by the same procedure as the proteoliposomes with the only difference that no rOCT1 protein was added.

Uptake and Efflux Measurements in Proteoliposomes. For uptake measurements, proteoliposomes filled with KC buffer were preincubated for 10 min at 37 °C in the absence or presence of 20 μM valinomycin. The preincubation was performed with 100 μM quinine, an inhibitor of rOCT1, or without quinine. Uptake was initiated by mixing 10 μL of prewarmed proteoliposomes (37 °C) with 90 μL of prewarmed (37 °C) transport medium consisting of (i) KC buffer, (ii) NaC buffer (20 mM imidazole, pH 7.4, 0.1 mM magnesium cyclamate, 100 mM sodium cyclamate), (iii) mixtures of KC and NaC buffer, or (iv) 20 mM imidazole, pH 7.4, and 0.1 mM magnesium cyclamate plus either 100 mM lithium cyclamate, 100 mM cesium cyclamate, or 100 mM lysine cyclamate. The transport media contained 12 nM [^{3}H]MPP plus the indicated concentrations of unlabeled MPP. Uptake was stopped by adding 1 mL of ice-cold stop solution (KC buffer containing 100 μM quinine). For measurement of radioactivity within proteoliposomes, the proteoliposomes suspended in stop solution were applied to 0.22 μm cellulose acetate filters (Millipore GSWP) and washed with 10 mL of ice-cold stop solution. The filters were dissolved in LUMASAFE PLUS cocktail (Lumac LSC, Groningen, The Netherlands) and assayed for radioactivity. The data were corrected for nonspecific binding of [^{3}H]MPP to the filters.

To measure *trans* stimulation of MPP uptake, 150 μL proteoliposomes were mixed with 150 μL of KC buffer containing either 5 or 0.2 mM choline cyclamate. Samples were preincubated for 60 min at 25 °C in the presence of 20 μM valinomycin. Uptake at 37 °C was started by mixing 20 μL of prewarmed proteoliposomes with 480 μL of prewarmed transport medium consisting of KC buffer supplemented with 0.1 mM choline cyclamate, 0.1 μM [^{3}H]MPP, and 20 μM valinomycin. For measurements in the presence of quinine, 100 μM quinine was added to the transport media. Uptake was stopped after 1 s incubation by adding ice-cold stop solution, and radioactivity in the proteoliposomes was determined.

To measure *trans* stimulation of MPP efflux by extracellular choline, 300 μL of proteoliposomes was preincubated with 0.1 μM [^{3}H]MPP and 20 μM valinomycin for 15 min at 37 °C. Quinine was added to a part of the proteoliposomes to a final concentration of 100 μM and incubated for another 5 min at 37 °C. Efflux was started by mixing 10 μL of the proteoliposomes with 190 μL of KC buffer prewarmed to 37 °C with or without 10 mM choline, and each with or without 100 μM quinine. Efflux was stopped after 1 s, and radioactivity in the proteoliposomes was measured.

Calculation and Statistics. Data are presented as mean values ± standard deviations (SD) from three to five individual measurements (Figures 2a, 3, and 5) or from three to five measurements, each, performed in the absence or presence of quinine (Figures 2b, 6, 7, 8, and 9). In Figures 2, 3, 5, and 7 typical experiments out of three are presented. The experiments shown in Figures 6 and 10 were reproduced once. Michaelis−Menten constant (K_m) values and maximal transport velocities (V_{max}) were calculated by fitting the Michaelis−Menten equation to the quinine-sensitive uptake rates measured at eight different substrate concentrations. IC_{50} values were calculated by fitting the Hill equation for multisite inhibition to uptake rates measured in the presence of seven to ten different inhibitor concentrations. Linear regression was employed to fit the potential dependence of

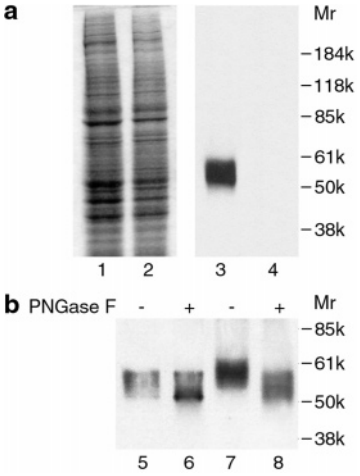

FIGURE 1: Detection of glycosylated rOCT1 protein in plasma membranes of Sf9 cells. (a) Detection of rOCT1 protein in crude membranes isolated from Sf9 cells transfected with rOCT1. Transfected (lanes 1 and 3) and nontransfected Sf9 cells (lanes 2 and 4) were homogenized and the proteins separated by SDS−PAGE. Coomassie Brilliant Blue staining (lanes 1 and 2) and Western blot for rOCT1 (lanes 3 and 4) are shown. (b) N-Glycosylation of rOCT1 in the plasma membrane of Sf9 cells in transfected Sf9 cells. Crude membranes (lanes 5 and 6) or enriched plasma membranes (lanes 7 and 8) of transfected Sf9 cells were incubated without or with PNGase F, separated by SDS−PAGE, and analyzed for rOCT1 by Western blotting. Per lane, 5 μg of protein was applied.

MPP uptake by rOCT1. For comparison of mean values, unpaired two-sided Student's *t*-test was used. Statistical calculations and curve fitting were done with GraphPad 4.0 (San Diego, CA).

RESULTS

Expression of rOCT1 in Sf9 Cells. Insect Sf9 cells were transfected with recombinant baculovirus expressing rOCT1. Four days after transfection, the cells were harvested and analyzed for expression of rOCT1 by Western blotting or by measuring the uptake of [^{3}H]MPP. In Figure 1a, crude membranes isolated from Sf9 cells without and with transfection of rOCT1 were separated by SDS−PAGE and either stained with Coomassie Brilliant Blue (lanes 1 and 2) or blotted to polyvinylidene difluoride membrane and stained with an antibody against the extracellular loop of rOCT1 (lanes 3 and 4) (*21*). In the Coomassie staining of crude membranes no difference between nontransfected control cells and rOCT1-transfected cells could be seen. However, in Western blots of the transfected cells, a broad band at ~55 Da was stained by an affinity-purifed antibody against rOCT1. To investigate whether the rOCT1 protein expressed in Sf9 cells was glycosylated, we compared the migration of rOCT1 from crude membranes versus enriched plasma membranes and performed N-deglycosylation with PNGase F (Figure 1b). rOCT1 from enriched plasma membranes migrated slower in SDS−PAGE than rOCT1 from crude membranes. This suggests that the crude membrane fraction contains a relatively large amount of endoplasmic reticulum with unglycosylated or incompletely glycosylated rOCT1. After deglycosylation, the migration of rOCT1 was faster. With enriched plasma membranes, this shift of molecular mass was more pronounced than with the crude membranes.

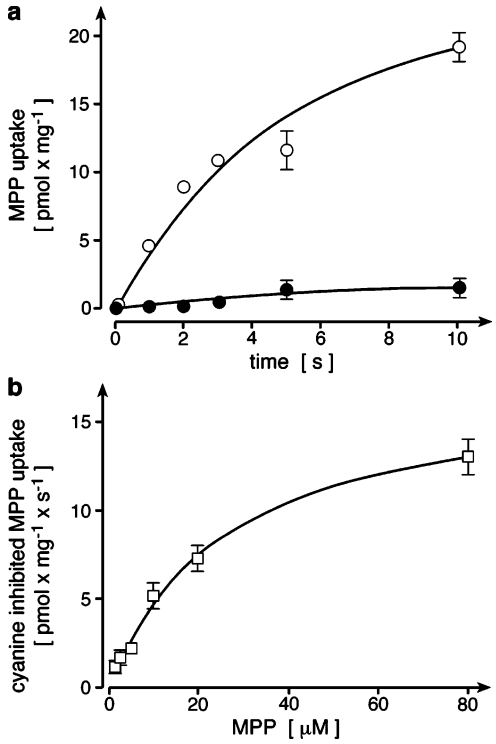

FIGURE 2: MPP uptake by Sf9 cells expressing rOCT1. (a) Time course of [^{3}H]MPP (10 μM) uptake in the absence (○) and presence (●) of 75 μM cyanine863. (b) Concentration dependence of cyanine863-inhibited MPP uptake. Cells were incubated for 1 s in the absence and presence of 75 μM cyanine863 with various concentrations of [^{3}H]MPP, and cyanine863-inhibited uptake rates were calculated. The Michaelis−Menten equation was fitted to the data. A typical experiment is shown. The data indicate expression of functionally active rOCT1 in insect cells.

The data show that rOCT1 is expressed in Sf9 cells, targeted to the plasma membrane, and N-glycosylated.

Functional Characterization of Organic Cation Transport in Sf9 Cells Expressing rOCT1. Four days after transfection of Sf9 cells with pAc360Myc-rOCT1-His, uptake of 10 μM [^{3}H]MPP was measured at 30 °C in the absence and presence 75 μM cyanine863 (*4*) and compared with uptake of nontransfected control cells. After 1 s, cyanine863-inhibited uptake rates of 4.6 ± 0.6 and 1.2 ± 0.2 pmol (mg of protein)$^{-1}$ s^{-1} were obtained for cells expressing rOCT1 and nontransfected cells, respectively (mean ± SD, $n = 6$ each group, $P < 0.001$ for difference). The data indicate significant expression of organic cation uptake by rOCT1. They also show some endogeneous cyanine863-inhibitable MPP uptake in the Sf9 cells, apparently mediated by an organic cation transporter that is not detected by our antibody against rOCT1. Figure 2a shows the time course of MPP (10 μM) uptake in cells expressing rOCT1 in the absence and presence of 75 μM cyanine863. The data show that the cyanine863-inhibited MPP uptake was linear for about 2 s. Using 1 s incubation in Sf9 cells expressing rOCT1, cyanine863-inhibited uptake of [^{3}H]MPP had a K_m of 25 ± 7 μM MPP and a V_{max} of 12.1 ± 3.7 pmol mg^{-1} s^{-1} (mean ± SD, $n =$ 3). A typical experiment is shown in Figure 2b. The K_m values for MPP uptake measured after expression of rOCT1 in other cell types were in the same range, namely, 3−19 μM in oocytes of *X. laevis* (*9*) and 14 ± 4 μM in human embryonic kidney (HEK) 293 cells (H. Koepsell and I. Schatz, unpublished data).

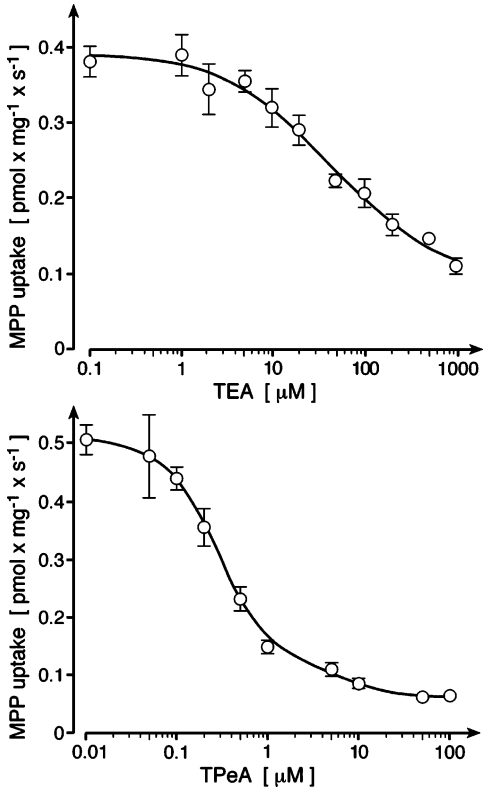

FIGURE 3: Inhibition of MPP uptake in rOCT1 expressing Sf9 cells by TEA (upper panel) and TPeA (lower panel). Cells were incubated for 1 s with 0.1 μM [^{3}H]MPP in the absence of inhibitors or in the presence of the indicated inhibitor concentrations, and the uptake of radioactivity was measured. The Hill equation was fitted to the data. Typical experiments are shown. The data indicate that rOCT1 expressed in Sf9 cells has similar affinities for TEA and TPeA compared to rOCT1 expressed in *Xenopus* oocytes or mammalian cells.

To determine the affinity of tetraethylammonium (TEA) and tetrapentylammonium (TPeA) to rOCT1 expressed in Sf9 cells, we measured the uptake of 0.1 μM [^{3}H]MPP in the presence of various concentrations of TEA or TPeA (Figure 3). TEA (1 mM) or 100 μM TPeA inhibited the uptake of 0.1 μM [^{3}H]MPP by 72% and 89%, respectively. The half-maximal inhibitor concentrations (IC_{50} values) were 44 $\pm$ 15 μM for TEA and 0.23 $\pm$ 0.01 μM for TPeA (mean $\pm$ SD, $n = 3$). Since the concentration of MPP used for these measurements was more than 100-fold below the K_m for MPP, the obtained IC_{50} values are identical with the K_i values. After expression of rOCT1 in oocytes of *X. laevis* or in HEK 293 cells, we obtained similar IC_{50} values for TEA [oocytes: 115 μM (*14*)] and TPeA [HEK 293 cells: 0.18 μM (*13*)].

Purification of rOCT1 from Sf9 Cells. Three days after transfection of Sf9 cells with recombinant baculovirus, cells from ten 14.5 cm diameter culture plates were lysed and membrane proteins solubilized by 1 h incubation at 4 °C with 1% (w/v) CHAPS. Nonsolubilized material was removed by 1 h centrifugation at 100000*g* (protein content of supernatant: 42 $\pm$ 7 mg, mean $\pm$ SD of three independent experiments). Next, glycosylated rOCT1 protein was enriched by absorption on lentil−lectin Sepharose beads and elution with 300 mM methyl α-D-mannopyranoside (Figure 4, lanes 3 and 4). The eluate contained 1.6 $\pm$ 0.3 mg of glycosylated proteins. The final purification of His-tagged

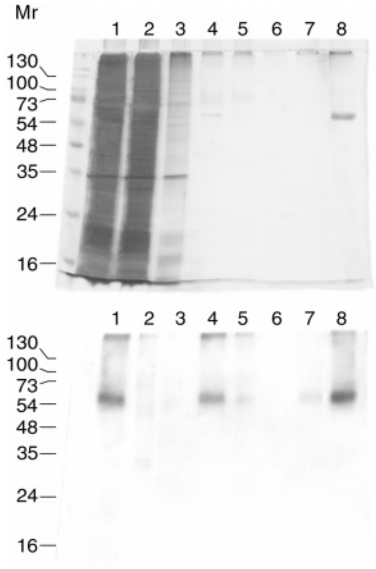

FIGURE 4: Purification of histidine-tagged rOCT1 expressed in Sf9 cells. rOCT1 was purified by affinity purification on lentil−lectin Sepharose and Ni^{2+}-NTA−agarose. Samples from various purification steps were separated by SDS−PAGE and silver-stained (upper panel) or analyzed by Western blotting with an antibody against rOCT1 (lower panel). Lane 1: supernatant (20 mL) obtained after 1 h centrifugation at 100000*g* of Sf9 cells that were solubilized with CHAPS (lysis buffer). Lentil−lectin Sepharose beads were added to this supernatant. Lane 2: flow-through (20 mL) obtained after the suspended lentil−lectin Sepharose beads were filled into a column. Lane 3: eluate (20 mL) obtained after the column was washed with lysis buffer. Lane 4: eluate (20 mL) obtained after the column was washed with lysis buffer containing 300 mM methyl α-D-mannopyranoside to elute glycosylated proteins. To this eluate were added Ni^{2+}-NTA−agarose beads to bind histidine-tagged rOCT1. Lane 5: flow-through (20 mL) that was obtained after the suspended Ni^{2+}-NTA−agarose beads were filled into a column. Lane 6: eluate (5 mL) obtained after the Ni^{2+}-NTA−agarose beads were washed with lysis buffer containing 5 mM imidazole. Lane 7: eluate (5 mL) obtained with lysis buffer containing 20 mM imidazole. Lane 8: eluate (one of three 0.3 mL fractions with protein) obtained with 50 mM imidazole. Per lane, 20 μL of the above-described samples was applied. The data indicate purification of rOCT1.

rOCT1 was performed by affinity chromatography on Ni^{2+}-NTA−agarose beads (Figure 4, lanes 5−8). Bound rOCT1 was eluted with 50 mM imidazole. A single protein band was detectable in a silver-stained SDS−polyacrylamide gel of the eluate. It was identified as rOCT1 by Western blotting. The ~40 mg of protein in the 100000*g* supernatant of the CHAPS-lysated Sf9 cells yielded 71 $\pm$ 4 μg (mean $\pm$ SD of the three independent experiments) of purified rOCT1 protein, corresponding to 0.17% of the protein in the 100000*g* supernatant.

Demonstration of Organic Cation Transport in Proteoliposomes Containing Purified rOCT1. Purified rOCT1 was reconstituted into proteoliposomes that contained 100 mM potassium cyclamate. Uptake of MPP was measured after incubation of the proteoliposomes at 37 °C with 0.1 μM [^{3}H]-MPP in the presence of 10 mM potassium cyclamate and 90 mM sodium cyclamate. The uptake measurements were performed in the absence and presence of 100 μM quinine, an inhibitor of rOCT1 (Figure 5). Significant quinine-inhibited uptake of MPP was obtained when the measurements were performed in the presence of the potassium ionophore valinomycin. This uptake was linear for about 1

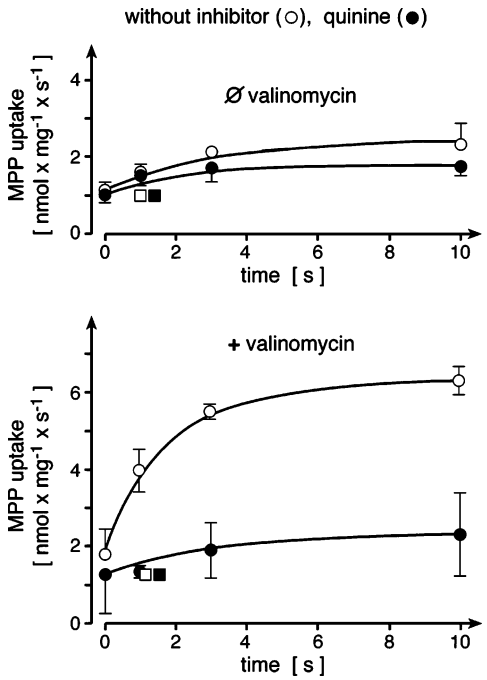

FIGURE 5: Time course of MPP uptake by proteoliposomes containing purified rOCT1 protein, inhibition by quinine, and stimulation by membrane potential. Purified rOCT1 was reconstituted in proteoliposomes containing 20 mM imidazole cyclamate, pH 7.4, 0.1 mM magnesium cyclamate, and 100 mM potassium cyclamate (KC buffer) (circles). In addition, liposomes were formed without addition of rOCT1 protein (squares). Transport measurements were performed in the absence of valinomycin (upper panel) or in the presence of valinomycin (lower panel). Uptake of MPP was measured in the absence (○, □) or presence (●, ■) of 100 μM quinine. Proteoliposomes or liposomes were incubated at 37 °C with 20 mM imidazole cyclamate, pH 7.4, 1 mM magnesium cyclamate, 90 mM sodium cyclamate, and 10 mM potassium cyclamate containing 0.1 μM [^{3}H]MPP. After various time intervals, uptake was stopped, the proteoliposomes or liposomes were washed on filters, and the radioactivity was analyzed. The data show quinine-inhibited MPP uptake by reconstituted rOCT1 in the presence of an inside negative potassium diffusion potential.

s. Valinomycin allowed the efflux of potassium and induced an inside negative diffusion potential that could not be compromised by the impermeant anion cyclamate used in this system. In control experiments we measured the uptake of 0.1 μM [^{3}H]MPP into liposomes that were generated without addition of rOCT1 protein. With these liposomes no significant quinine-inhibited uptake of MPP could be detected in the absence or presence of valinomycin (see, for example, Figure 5). We also measured the initial uptake of 20 μM [^{14}C]TEA in the presence of valinomycin into proteoliposomes that were reconstituted with purified rOCT1 protein. With 100 mM potassium cyclamate in the incubation medium (symmetric potassium) and with 90 mM sodium cyclamate plus 10 mM potassium cyclamate in the incubation medium (outwardly directed 9-fold potassium gradient) uptake rates of 6 ± 3 and 68 ± 4 nmol mg^{-1} s^{-1} were obtained, respectively (mean ± SD from five measurements each, $P < 0.01$ for difference). The data show that purified rOCT1 mediates potential dependent uptake of MPP and TEA and does not require additional proteins for this function. Previous demonstrations of cation uptake after expression of OCT transporters in oocytes of *X. laevis* and in cultured cells (*4*−*11*, *23*) did not exclude this possibility. Note that the uptake measurements in the proteoliposomes were performed in the absence of chloride, phosphate, and sulfate and of organic anions such as succinate or α-ketoglutarate, which are countertransported substrates of the organic anion transporters of the *SLC22* family (*3*). This shows that these ions are not required for organic cation transport by rOCT1.

Potential Dependence of MPP Transport in Proteoliposomes. We characterized the potential dependence of organic cation uptake by purified and reconstituted rOCT1, measuring initial rates for the quinine-inhibited uptake of 0.1 μM [^{3}H]MPP into proteoliposomes at various membrane potentials. Inside negative potassium diffusion potentials were generated by applying various initial outwardly directed potassium gradients in the presence of the potassium ionophore valinomycin and the impermeant anion cyclamate. For uptake measurements proteoliposomes containing KC buffer with 100 mM potassium cyclamate were incubated with 0.1 μM [^{3}H]MPP in KC buffer or various mixtures of NaC buffer and KC buffer. The membrane potential was calculated using the Nernst equation. Figure 6a shows that quinine-inhibited MPP uptake rate increased about 10-fold when the membrane potential was changed from 0 to −100 mV. No significant quinine-inhibited uptake of MPP was resolved at 0 mV.

Figure 6b shows an experiment where we investigated whether the quinine-inhibited uptake of MPP at −61 mV was dependent on inorganic cations on the *cis* side. Proteoliposomes containing 100 mM potassium cyclamate were preincubated with valinomycin, and quinine-inhibited uptake of 0.1 μM [^{3}H]MPP uptake was measured in the presence of 10 mM potassium cyclamate plus either 90 mM sodium cyclamate, 90 mM lithium cyclamate, 90 mM cesium cyclamate, or 90 mM lysine cyclamate. With these four cations, similar quinine-inhibited uptake rates of MPP were obtained. In Figure 6c we measured quinine-inhibited uptake of 0.1 μM [^{3}H]MPP in the presence of different sodium concentrations in the incubation buffer replacing sodium by lysine. Measurements were performed at a calculated initial membrane potential of −61 mV (100 mM potassium in the liposomes, 10 mM potassium in the incubation buffer, presence of valinomycin). No effect of sodium on MPP uptake was observed. The data in Figure 6b,c indicate that MPP uptake by rOCT1 is independent from sodium, lithium, or cesium on the *cis* side.

To determine whether the uptake of MPP by rOCT1 is pH dependent, we measured quinine-inhibited uptake after 1 s incubation of proteoliposomes with 0.1 μM [^{3}H]MPP at pH 7.4 (standard condition), pH 6.4, or pH 8.4. The measurements were performed at an initial calculated membrane potential of −61 mV (100 mM potassium cyclamate in the liposomes, 10 mM potassium cyclamate plus 90 mM sodium cyclamate in the incubation buffer, presence of valinomycin). The obtained MPP uptake rates were not significantly different at different pH [pH 7.4, 100 ± 20%; pH 6.4, 94 ± 6%; pH 8.4, 96 ± 2% ($n = 3$)].

Substrate Dependence and Inhibitor Sensitivity of MPP Transport in Proteoliposomes. Substrate dependence of quinine-inhibited MPP uptake was measured at a calculated potassium diffusion potential of −61 mV. Figure 7 shows a typical experiment. A hyperbolic dependence of MPP uptake on MPP concentration was observed, with an apparent K_m of 30 ± 17 μM and a V_{max} of 324 ± 68 nmol mg^{-1} s^{-1} (mean ± SD of three independent experiments). The K_m

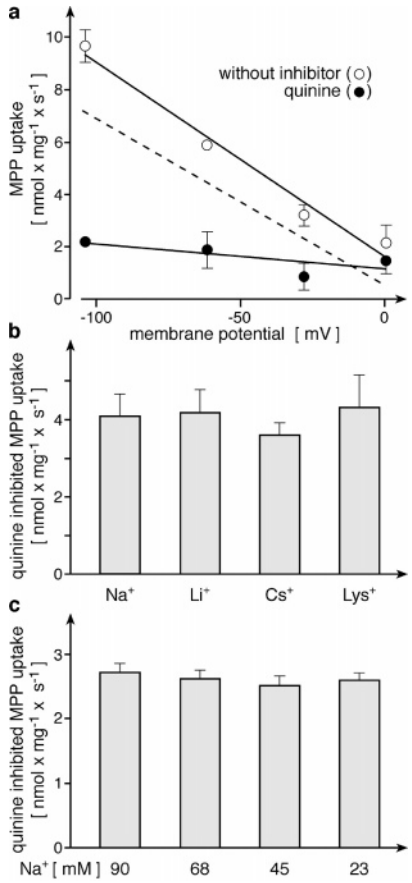

FIGURE 6: MPP uptake by reconstituted rOCT1 at various membrane potentials, in the presence of various monovalent cations, and in the presence of different sodium concentrations. Purified rOCT1 was reconstituted in proteoliposomes which contained 100 mM potassium cyclamate as in Figure 5. Uptake of MPP was measured in the presence of valinomycin at 37 °C in the absence (○) and presence of 100 μM quinine (●), and the quinine-inhibited uptake rates were calculated [dotted line in (a), columns in (b) and (c)]. (a) Potential dependence of MPP uptake. Proteoliposomes containing KC buffer with 100 mM potassium cyclamate were incubated for 1 s with 0.1 μM [^{3}H]MPP dissolved in 20 mM imidazole cyclamate, pH 7.4, and 0.1 mM magnesium cyclamate plus either (i) 98 mM sodium cyclamate and 2 mM potassium cyclamate, (ii) 90 mM sodium cyclamate and 10 mM potassium cyclamate, (iii) 75 mM sodium cyclamate and 25 mM potassium cyclamate, or (iv) 100 mM potassium cyclamate. The equilibrium potassium diffusion potentials (E_m) were calculated by the Nernst equation ($E_m = -61 \log [K^+]_{inside}/[K^+]_{outside}[V]$). For MPP uptake in the presence of quinine no signifcant potential dependence was observed. (b) Quinine-inhibited MPP uptake in the presence of a fixed potassium diffusion potential and different monovalent cations. Proteoliposomes containing KC buffer with 100 mM potassium cyclamate were incubated for 1 s with 0.1 μM [^{3}H]MPP dissolved in 20 mM imidazole cyclamate, pH 7.4, 0.1 mM magnesium cyclamate, and 10 mM potassium cyclamate plus either 90 mM sodium cyclamate (Na^+), 90 mM lithium cyclamate (Li^+), 90 mM cesium cyclamate (Cs^+), or 90 mM lysine cyclamate (Lys^+). (c) Quinine-inhibited MPP uptake in the presence of a fixed potassium diffusion potential and different concentrations of extracellular sodium. Proteoliposomes containing KC buffer were incubated for 1 s with 0.1 μM [^{3}H]MPP dissolved in 20 mM imidazole cyclamate, pH 7.4, and 0.1 mM magnesium cyclamate containing 10 mM potassium cyclamate plus either 90 mM sodium cyclamate, 68 mM sodium cyclamate plus 22 mM lysine cyclamate, 45 mM sodium cyclamate plus 45 mM lysine cyclamate, or 23 mM sodium cyclamate plus 67 mM lysine cyclamate. The data indicate that MPP uptake by rOCT1 is strongly dependent on the membrane potential, independent from inorganic monovalent cations and independent from the extracellular sodium concentration.

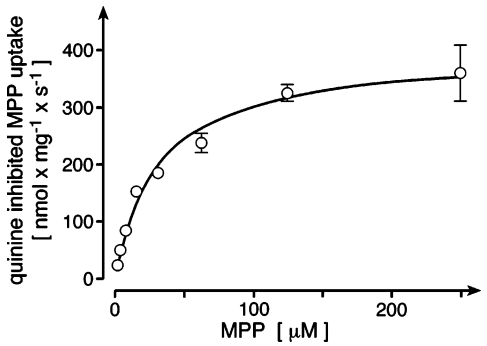

FIGURE 7: Concentration dependence of quinine-inhibited MPP uptake by proteoliposomes containing purified rOCT1 at −61 mV. Purified rOCT1 was reconstituted in proteoliposomes as in Figure 5. Quinine-inhibited uptake of [^{3}H]MPP in the presence of various concentrations of unlabeled MPP was measured after 1 s inubation at 37 °C. The measurements were performed in the presence of valinomycin with 100 mM potassium cyclamate inside the proteoliposomes and 10 mM potassium cyclamate plus 90 mM sodium cyclamate in the incubation buffer. The Michaelis−Menten equation was fitted to the data. A typical experiment is shown. The K_m value calculated for this experiment was 32 ± 5 μM. The data indicate substrate saturation of MPP uptake by reconstituted rOCT1.

value is similar to the K_m value measured in intact insect cells, indicating functional integrity of rOCT1 after purification and reconstitution. The relatively large variation of the K_m value observed between individual experiments is not understood. We have previously observed a large variation of the K_m values for MPP after expression of rOCT1 in different batches of oocytes from *X. laevis* (*9*). Remarkably, the V_{max} value related to protein measured for MPP uptake in proteoliposomes was more than 20000 times higher than the V_{max} value measured in the insect cells. This value probably overestimates the degree of purification because uptake measurements in intact cells reflect the activity of rOCT1 protein within the plasma membrane whereas reconstituted rOCT1 protein was derived from plasma membrane and intracellular compartments. From the V_{max} value for MPP uptake in proteoliposomes a minimum turnover of 20 s^{-1} can be calculated. The actual turnover is supposed to be much higher because our preparation probably contains a large fraction of denatured rOCT1 protein and/or of rOCT1 that is not reconstituted properly. In addition, part of the proteoliposomes may be multilamellar or leaky and may not contribute to measured transport activity. Finally, the orientation of rOCT1 in the proteoliposomes is not known, and the turnover for rOCT1-mediated organic cation transport across the membrane may be different depending on the direction of transport (*12*).

To estimate the affinity of another substrate and of two inhibitors of rOCT1, we measured the inhibition of [^{3}H]MPP uptake (0.1 μM) by various concentrations of TEA, tetrabutylammonium (TBuA), and TPeA. The concentration inhibition curves in Figure 8 show that 88% of MPP uptake was inhibited by 10 mM TEA, 83% by 0.1 mM TBuA, and 85% by 0.1 mM TPeA. The calculated IC_{50} values were 197 ± 11 μM for TEA, 19 ± 1 μM for TBuA, and 1.75 ± 0.03 μM for TPeA. Because the concentration of 0.1 μM MPP used for the uptake measurements was more than 100 times below the K_m value for MPP, the IC_{50} values are approximately identical to the K_i values. The IC_{50} value for TEA inhibition of MPP uptake was similar in proteoliposomes and in oocytes of *X. laevis* expressing rOCT1 (115

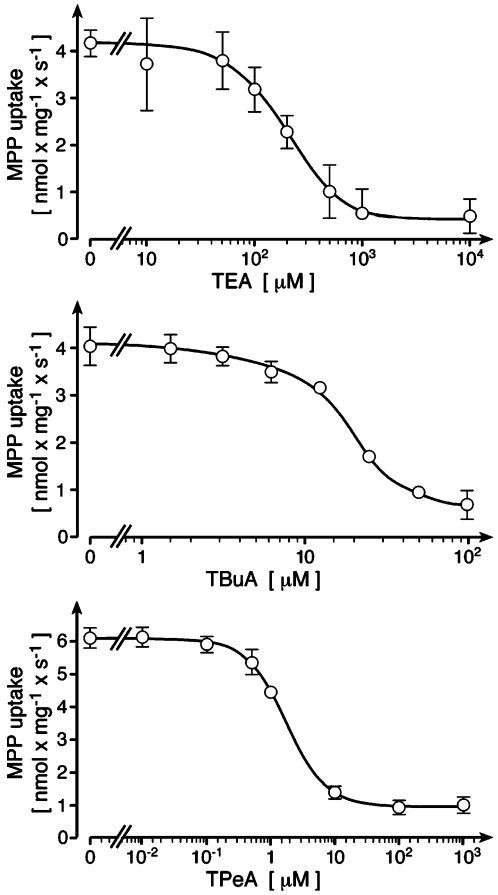

FIGURE 8: Concentration dependence for inhibition of MPP uptake into proteoliposomes by TEA, TBuA, or TPeA. Purified rOCT1 was reconstituted in proteoliposomes, and uptake of 0.1 μM [^{3}H]-MPP was measured for 1 s at 37 °C in the presence of valinomycin. Proteoliposomes were filled with 100 mM potassium cyclamate, and the incubation buffer contained 10 mM potassium cyclamate plus 90 mM sodium cyclamate. Uptake was measured in the presence of the indicated concentrations of TEA (upper panel), TBuA (middle panel), or TPeA (lower panel). In the presence of 100 μM quinine 93% of MPP uptake was inhibited. The Hill equation was fitted to the data. The data indicate reduced affinity of TEA and TPeA to purified and reconstituted rOCT1 as compared with Sf9 cells expressing rOCT1. At variance, the affinity of TEA to reconstituted rOCT1 was similar, compared to rOCT1 expressed in *Xenopus* oocytes or mammalian cells.

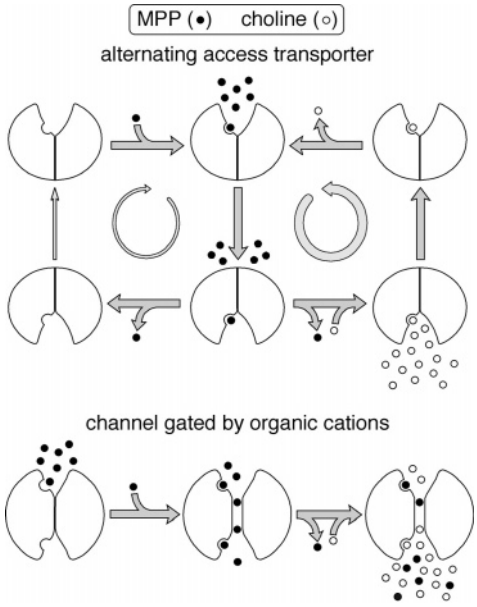

FIGURE 9: Models describing OCT1 as the alternating access transporter or channel that is gated by organic cations. Both models were consistent with previous observations such as (i) symmetric flux of organic cations (*1*), (ii) substrate saturation for transport in both directions (*1*), (iii) ligand-inducable conformational changes (*24*), (iv) potential dependence of cation transport (*1*), (v) binding of organic cations from the extracellular and intracellular side of the plasma membrane (*12*), and (vi) a channel-like selectivity filter (*24*). For both models the presumed effects of choline (open circles) on the uptake of MPP (closed circles) are depicted. The *trans* stimulation of rOCT1-mediated MPP uptake by choline observed in the present paper is consistent with the alternating access transporter model but difficult to reconcile with the channel model.

μM; see Table 2 in ref *14*); however, they were 4.5 times higher than in intact Sf9 cells expressing rOCT1. Similarly, the IC_{50} value for TPeA inhibition of MPP uptake in proteoliposomes was 7.6 times higher compared with intact Sf9 cells.

Trans Stimulation of MPP Uptake in Proteoliposomes. The OCTs have been described as facilitative diffusion systems that translocate a variety of different organic cations in either direction and utilize substrate concentration gradients and membrane potential as driving forces (*5*, *7*, *8*). Substrate binding regions with overlapping binding sites for different substrates and/or inhibitors have been identified that are accessible from the extracellular and intracellular side (*12*, *15*). It was shown that TBuA, a competitive inhibitor, has different affinities to rOCT2 at the extracellular versus the intracellular side (*12*). On the other hand, we recently detected that rOCT2 has channel-like properties in addition to substrate binding sites (*24*). Thus, the functional data with OCTs obtained so far are consistent with an "alternating access" transporter model (Figure 9, upper panel) and a channel that is gated by the binding of organic cations (Figure 9, lower panel). In the alternating access transporter model, a *trans* stimulation of cation uptake is expected if the reorientation of the empty transporter from the *trans* to the *cis* side is slower compared to the *trans*−*cis* reorientation of the substrate-loaded transporter. Strong *trans* stimulation is also expected for an antiporter but is difficult to reconcile with passive diffusion through a channel (Figure 9, lower panel).

To obtain information on the transport mechanism of rOCT1, we investigated the *trans* effects of choline on quinine-inhibitable uptake of [^{3}H]MPP in proteoliposomes as well as the *trans* effects of choline on quinine-inhibitable efflux of [^{3}H]MPP. The measurements were performed with clamped membrane potential to avoid indirect effects that may be induced by changes of membrane potential after addition of cationic substrate to the *trans* side. Voltage was clamped to 0 mV by performing the measurements with 100 mM potassium on both sides of the membrane in the presence of the potassium ionophore valinomycin. For uptake measurements, proteoliposomes containing KC buffer were preloaded with 0.1 mM or 2.5 mM choline and incubated for 1 s in KC buffer containing 0.1 μM [^{3}H]MPP plus 0.1 mM choline. The incubation was performed in the absence or presence of 100 μM quinine, and the quinine-inhibited uptake was determined. In two experiments we observed a 2.5-fold ($P < 0.05$ for difference) and 3-fold stimulation of MPP uptake (Figure 10a, $P < 0.01$ for difference) by 2.5 versus 0.1 mM choline inside the proteoliposomes.

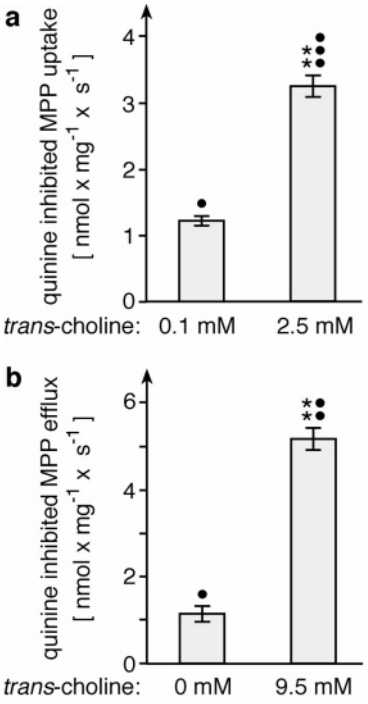

FIGURE 10: *Trans* stimulation of MPP uptake by purified rOCT1 reconstituted into proteoliposomes measured with a clamped membrane potential. Purified rOCT1 was reconstituted in proteoliposomes, and uptake or efflux of [^{3}H]MPP was measured at 37 °C and at 0 mV (valinomycin with 100 mM potassium cyclamate inside the proteoliposomes as well as in the incubation media). Quinine- (100 μM) inhibited MPP uptake is shown (mean ± SD from five measurements, each). (a) *Trans* stimulation of MPP uptake by 2.5 mM choline (in) versus 0.1 mM choline (out). Proteoliposomes containing KC buffer were preincubated for 60 min at 25 °C with KC buffer containing either 0.1 or 2.5 mM choline cyclamate. Uptake of MPP was measured after 1 s incubation with KC buffer containing 0.1 μM [^{3}H]MPP plus 0.1 mM choline. (b) *Trans* stimulation of MPP efflux by 9.5 mM choline. Proteoliposomes containing KC buffer were preincubated for 15 min (37 °C) with KC buffer containing 0.1 μM [^{3}H]MPP. The proteoliposomes were incubated for 1 s in KC buffer without choline or in KC buffer containing 9.5 mM choline, and efflux was analyzed by measuring [^{3}H]MPP in the proteoliposomes. Key: **, $P < 0.01$ for the difference between choline concentrations on the *trans* side; •, $P < 0.05$; ••, $P < 0.01$; •••, $P < 0.001$ for the difference between uptake in the absence and presence of 100 μM quinine.

Because the observed *trans* stimulation might theoretically be due to inhibition of [^{3}H]MPP back-flux by a high concentration of choline in the proteoliposomes (*25*), we also tested whether efflux of [^{3}H]MPP from proteoliposomes could be *trans* stimulated by choline. In this experimental setting, back-flux of [^{3}H]MPP can be neglected because [^{3}H]-MPP leaving the proteoliposomes is diluted in a large volume. For efflux measurements, proteoliposomes were preloaded with 0.1 μM [^{3}H]MPP and incubated in KC buffer or KC buffer containing 9.5 mM choline. Quinine-inhibitable efflux of [^{3}H]MPP was measured after 1 s incubation. In one experiment, a 3-fold *trans* stimulation by choline stimulation of MPP efflux by choline ($P < 0.05$ for difference) and in a second experiment (Figure 10b) a 4-fold *trans* stimulation was observed ($P < 0.01$ for difference).

The *trans* stimulation experiments suggest that rOCT1 operates as an alternating access transporter. Because the orientation of rOCT1 in the proteoliposomes has not been defined, we do not know whether the observed *trans* stimulation is valid for uptake of organic cations into cells, for cellular organic cation release, or for organic cation translocation in either direction.

DISCUSSION

In this work, we report procedures to purify glycosylated rOCT1 protein expressed in insect cells, to reconstitute the purified protein into proteoliposomes, and to measure rOCT1-mediated transport of organic cations into proteoliposomes. Although the yield of purified rOCT1 protein was relatively low (70 μg from 10 standard culture plates), in line with previous reports of purification of transporters and receptors (*26*−*28*), we were able to reconstitute functional protein into proteoliposomes and to measure transport activity by rOCT1. Our reconstitution procedure was optimized for the reconstitution of small amounts of a transporter (*22*). Protein−lipid aggregates were formed by detergent removal from a mixture of purified rOCT1 plus lipids, and the aggregated material was reconstituted by mixing it with multilamellar liposomes formed from phosphatidylserine and cholesterol and by freezing and thawing. In addition to allowing the handling of small amounts of protein, this procedure leads to the formation of large proteoliposomes that are rich in cholesterol and highly impermeant for ions (*22*). In such proteoliposomes, cation gradients persist for a relatively long time provided that a highly impermeant anion like cyclamate is used. For example, for the Na^+-D-glucose cotransporter SGLT1 reconstituted into these type of proteoliposomes, sodium-gradient-driven glucose uptake was measured that was linear for minutes (*22*). The present work shows that these proteoliposomes can also be used to measure transport activities of electrogenic transport systems that are driven by membrane potential. With initial outward gradients of potassium in the presence of the potassium ionophore valinomycin, potassium diffusion potentials were generated, revealing a potential dependent cation uptake of rOCT1 that was linear for about 1 s.

The transport measurements with purified and reconstituted rOCT1 protein reported in the present work increase the understanding of the function of organic cation transporters. First, the measurements indicate that rOCT1 is sufficient to mediate transport of organic cations. This has been tacitly assumed for organic cation transporters (OCTs) but has never been proven (*1*). Previously, organic cation transport by OCTs was characterized after expression of the transporters in various cell types. In these measurements, the theoretical possibility was not excluded that a widely expressed endogeneous protein, for example, an intracellular organic cation binding protein or a transporter subunit, is required for organic cation transport. Second, we showed that rOCT1 translocates organic cations in the absence of physiological anions such as chloride, phosphate, sulfate, α-ketoglutarate, or succinate because cyclamate was the only anion in our assay system. A similar result was previously reported for rOCT2 measuring organic cation-induced currents in voltage-clamped giant patches (*8*). In these measurements, rOCT2-mediated currents were induced by choline or TEA using chloride as the only anion. Note that the observation that rOCT1 mediates organic cation transport in the absence of physiological anions does not exclude the possibility that organic anions cause *cis* inhibition and/or *trans* stimulation of organic cation transport in vivo. For example, the organic anions α-ketoglutarate, *p*-aminohippurate, and probenecid

have been shown to be low-affinity *cis* inhibitors of organic cation transport by rOCT1 and rOCT2 (*9*), and some organic anion transporters of the *SLC22* family function as anion exchangers (*3*, *29*). Third, we showed that organic cation uptake by rOCT1 was independent from inorganic cations on the *cis* side. Quinine-inhibitable uptake of MPP at −60 mV was not significantly different whether 90 mM sodium, 90 mM lithium, 90 mM cesium, or 90 mM lysine was present on the *cis* side. Fourth, we demonstrate that organic cation uptake by rOCT1 is independent of proton gradients. Fifth, the present paper presents the first direct measurement of potential dependence of cation uptake by an organic cation transporter employing tracer flux experiments. In previous experiments performed with voltage-clamped oocytes, potential dependence of cation-induced currents rather than potential dependence of cation transport was demonstrated for rOCT1 (*7*), rOCT2 (*8*, *9*), rOCT3 (*10*), or hOCT2 (*30*). These measurements did not distinguish between effects of the membrane potential on organic cation translocation from effects on leakage of inorganic cations or countertransport of anions. In proteoliposomes containing rOCT1, quinine-inhibitable uptake of 0.1 μM [^{3}H]MPP measured at −100 mV was about 10 times higher than uptake measured at 0 mV. This pronounced potential dependence is supposed to be due to two additive effects: an acceleration of transporter reorientation and a hyperpolarization-induced decrease of the K_m value. In oocytes expressing rOCT1, the inward currents induced by superfusion of a saturating concentration of choline (10 mM) were two times higher at −100 mV compared to 0 mV (*7*) whereas the apparent affinity for choline decreased with more positive membrane potential. The half-maximal concentration for choline-induced current at −90 mV was 4-fold lower compared to −10 mV (*5*). Assuming that the K_m for MPP has the same potential dependence as the K_m value for choline, and taking the effects on apparent K_m and maximal induced current together, the potential dependence observed after reconstitution of rOCT1 appears to be similar to the potential dependence of choline-induced currents. Finally, we describe for the first time that uptake of an organic cation by an OCT transporter is *trans* stimulated by a transported substrate under voltage-clamp conditions. In previous experiments using oocytes and human embryonic kidney (HEK) 293 cells expressing rOCT1 or hOCT2, we observed that uptake and/or cellular efflux of [^{3}H]MPP was *trans* stimulated by some cationic substrates (*5*, *30*). Because membrane potential was not clamped in these experiments, we could not distinguish whether the observed *trans* stimulation reflected the underlying transport mechanism or resulted from membrane hyperpolarizaton by the cations added to the *trans* side. The *trans* stimulation of MPP uptake and of MPP efflux observed with voltage-clamped proteoliposomes indicates that rOCT1 cannot be a channel (Figure 9). A channel would implicate that the steep gradients of choline (2.5 mM inside > 0.1 mM outside during influx measurements, 9.5 mM outside > 0 mM inside during efflux measurements) inhibit the influx or efflux of [^{3}H]MPP, respectively, driven by the gentle gradients of MPP in the opposite directions (0.1 μM outside > 0 μM inside for influx, 0.1 μM inside > 0.5 nM outside for efflux). The observed *trans* stimulation is consistent with an alternating access transporter model in which the substrate binding site switches between an outwardly and an inwardly directed conformation and the reorientation of the loaded binding site is more rapid compared to reorientation of the empty site. In principle, *trans* stimulation is also consistent with an organic cation antiporter that would have to be electrogenic in the case of rOCT1; for example, this could be achieved by exchanging two monovalent cations against one monovalent cation. This model may be excluded on the basis of previous data with giant patches from oocytes expressing rOCT2 (*8*). With identical concentrations of choline on both sides, symmetrical currents were induced when the membrane potential was changed in opposite directions. So far, we cannot exclude the possibility that rOCT1 and rOCT2 employ different transport mechanisms. In addition, it is possible that rOCT2 and the other OCTs operate as electrogenic antiporters in vivo by exchanging different extracellular and intracellular cations. Using our reconstituted system, such questions cannot be answered because the orientation of rOCT1 in the proteoliposomes has not been defined. For this reason we do not know whether the observed *trans* stimulation of MPP influx and MPP efflux in proteoliposomes reflects rOCT1-mediated cation uptake into cells, cation efflux from cells, or cation transport in both directions.

The establishment of procedures to purify and reconstitute an organic cation transporter of the *SLC22* family and to measure potential dependent organic cation transport in proteoliposomes is an important step toward biophysical characterization and crystallization. Because the yield of purified rOCT1 protein from insect cells obtained so far is too low to prepare milligram amounts of protein economically, a further optimization of the expression conditions in insect cells is required (*31*, *32*). Using the described purification and reconstitution procedures, other expression systems will be explored to obtain a higher yield of purified and functional active transporter (*33*, *34*).

REFERENCES

1. Koepsell, H., Schmitt, B. M., and Gorboulev, V. (2003) Organic cation transporters, *Rev. Physiol., Biochem., Pharmacol. 150*, 36−90.
2. Koepsell, H. (2004) Polyspecific organic cation transporters: their functions and interactions with drugs, *Trends Pharmacol. Sci. 25*, 375−381.
3. Wright, S. H., and Dantzler, W. H. (2004) Molecular and cellular physiology of renal organic cation and anion transport, *Physiol. Rev. 84*, 987−1049.
4. Gründemann, D., Gorboulev, V., Gambaryan, S., Veyhl, M., and Koepsell, H. (1994) Drug excretion mediated by a new prototype of polyspecific transporter, *Nature 372*, 549−552.
5. Busch, A. E., Quester, S., Ulzheimer, J. C., Waldegger, S., Gorboulev, V., Arndt, P., Lang, F., and Koepsell, H. (1996) Electrogenic properties and substrate specificity of the polyspecific rat cation transporter rOCT1, *J. Biol. Chem. 271*, 32599−32604.
6. Gorboulev, V., Ulzheimer, J. C., Akhoundova, A., Ulzheimer-Teuber, I., Karbach, U., Quester, S., Baumann, C., Lang, F., Busch, A. E., and Koepsell, H. (1997) Cloning and characterization of two human polyspecific organic cation transporters, *DNA Cell Biol. 16*, 871−881.
7. Nagel, G., Volk, C., Friedrich, T., Ulzheimer, J. C., Bamberg, E., and Koepsell, H. (1997) A reevaluation of substrate specificity of the rat cation transporter rOCT1, *J. Biol. Chem. 272*, 31953−31956.
8. Budiman, T., Bamberg, E., Koepsell, H., and Nagel, G. (2000) Mechanism of electrogenic cation transport by the cloned organic cation transporter 2 from rat, *J. Biol. Chem. 275*, 29413−29420.
9. Arndt, P., Volk, C., Gorboulev, V., Budiman, T., Popp, C., Ulzheimer-Teuber, I., Akhoundova, A., Koppatz, S., Bamberg,

E., Nagel, G., and Koepsell, H. (2001) Interaction of cations, anions, and weak base quinine with rat renal cation transporter rOCT2 compared with rOCT1, *Am. J. Physiol. Renal Physiol. 281*, F454−F468.
10. Kekuda, R., Prasad, P. D., Wu, X., Wang, H., Fei, Y.-J., Leibach, F. H., and Ganapathy, V. (1998) Cloning and functional characterization of a potential-sensitive, polyspecific organic cation transporter (OCT3) most abundantly expressed in placenta, *J. Biol. Chem. 273*, 15971−15979.
11. Gründemann, D., Schechinger, B., Rappold, G. A., and Schömig, E. (1998) Molecular identification of the corticosterone-sensitive extraneuronal catecholamine transporter, *Nat. Neurosci. 1*, 349−351.
12. Volk, C., Gorboulev, V., Budiman, T., Nagel, G., and Koepsell, H. (2003) Different affinities of inhibitors to the outwardly and inwardly directed substrate binding site of organic cation transporter 2, *Mol. Pharmacol. 64*, 1037−1047.
13. Gorboulev, V., Volk, C., Arndt, P., Akhoundova, A., and Koepsell, H. (1999) Selectivity of the polyspecific cation transporter rOCT1 is changed by mutation of aspartate 475 to glutamate, *Mol. Pharmacol. 56*, 1254−1261.
14. Gorboulev, V., Shatskaya, N., Volk, C., and Koepsell, H. (2005) Subtype-specific affinity for corticosterone of rat organic cation transporters rOCT1 and rOCT2 depends on three different amino acids within the substrate binding region, *Mol. Pharmacol. 67*, 1612−1619.
15. Popp, C., Gorboulev, V., Müller, T. D., Gorbunov, D., Shatskaya, N., and Koepsell, H. (2005) Amino acids critical for substrate affinity of rat organic cation transporter 1 line the substrate binding region in a model derived from the tertiary structure of lactose permease, *Mol. Pharmacol. 67*, 1600−1611.
16. Valentin, M., Kühlkamp, T., Wagner, K., Krohne, G., Arndt, P., Baumgarten, K., Weber, W.-M., Segal, A., Veyhl, M., and Koepsell, H. (2000) The transport modifier RS1 is localized at the inner side of the plasma membrane and changes membrane capacitance, *Biochim. Biophys. Acta 1468*, 367−380.
17. O'Reilly, D. R., Miller, L. K., and Luckow, V. A. (1992) *Baculovirus expression vectors. A laboratory manual*, pp 51−93, W. H. Freeman and Co., New York.
18. King, L. A., and Possee, R. D. (1992) *The baculovirus expression system: A laboratory guide*, pp 124−126, Chapman and Hall, London.
19. Bradford, M. M. (1976) A rapid and sensitive method for the quantification of microgram quantities of protein utilizing the principle of protein-dye binding, *Anal. Biochem. 72*, 248−254.
20. Renes, J., DeVries, E. G. E., Nienhuis, E. F., Jansen, P. L. M., and Müller, M. (1999) ATP-and glutathione-dependent transport of chemotherapeutic drugs by the multidrug resistance protein MRP1, *Br. J. Pharmacol. 126*, 681−688.
21. Meyer-Wentrup, F., Karbach, U., Gorboulev, V., Arndt, P., and Koepsell, H. (1998) Membrane localization of the electrogenic cation transporter rOCT1 in rat liver, *Biochem. Biophys. Res. Commun. 248*, 673−678.
22. Koepsell, H., and Seibicke, S. (1990) Reconstitution and fractionation of renal brush border transport proteins, *Methods Enzymol. 191*, 583−605.
23. Mehrens, T., Lelleck, S., Çetinkaya, I., Knollmann, M., Hohage, H., Gorboulev, V., Boknik, P., Koepsell, H., and Schlatter, E. (2000) The affinity of the organic cation transporter rOCT1 is increased by protein kinase C-dependent phosphorylation, *J. Am. Soc. Nephrol. 11*, 1216−1224.
24. Schmitt, B. M., and Koepsell, H. (2005) Alkali cation binding and permeation in the rat organic cation transporter rOCT2, *J. Biol. Chem. 280*, 24481−24490.
25. Stein, W. D. (1990) *Channels, carriers, and pumps: An introduction to membrane transport*, pp 133−143, Academic Press, New York.
26. Reiländer, H., Boege, F., Vasudevan, S., Maul, G., Hekman, M., Dees, C., Hampe, W., Helmreich, E. J. M., and Michel, H. (1991) Purification and functional characterization of the human β_2-adrenergic receptor produced in baculovirus-infected insect cells, *FEBS Lett. 282*, 441−444.
27. Sievert, M. K., Thiriot, D. S., Edwards, R. H., and Ruoho, A. E. (1998) High-efficiency expression and characterization of the synaptic-vesicle monoamine transporter from baculovirus-infected insect cells, *Biochem. J. 330*, 959−966.
28. Guerini, D., Pan, B., and Carafoli, E. (2003) Expression, purification, and characterization of isoform 1 of the plasma membrane Ca^{2+} pump. Focus on calpain sensitivity, *J. Biol. Chem. 278*, 38141−38148.
29. Koepsell, H., and Endou, H. (2004) The SLC22 drug transporter family, *Pfluegers Arch. 447*, 666−676.
30. Busch, A. E., Karbach, U., Miska, D., Gorboulev, V., Akhoundova, A., Volk, C., Arndt, P., Ulzheimer, J. C., Sonders, M. S., Baumann, C., Waldegger, S., Lang, F., and Koepsell, H. (1998) Human neurons express the polyspecific cation transporter hOCT2, which translocates monoamine neurotransmitters, amantadine, and memantine, *Mol. Pharmacol. 54*, 342−352.
31. Miras, R., Cuillel, M., Catty, P., Guillain, F., and Mintz, E. (2001) Purification of heterologous sarcoplasmic reticulum Ca^{2+}-ATPase Serca1a allowing phosphoenzyme and Ca^{2+}-affinity measurements, *Protein Expression Purif. 22*, 299−306.
32. Werten, P. J. L., Hasler, L., Koenderink, J. B., Klaassen, C. H. W., de Grip, W. J., Engel, A., and Deen, P. M. T. (2001) Large-scale purification of functional recombinant human aquaporin-2, *FEBS Lett. 504*, 200−205.
33. Roosild, T. P., Greenwald, J., Vega, M., Castronovo, S., Riek, R., and Choe, S. (2005) NMR structure of Mistic, a membrane-integrating protein for membrane protein expression, *Science 307*, 1317−1321.
34. Klammt, C., Löhr, F., Schäfer, B., Haase, W., Dötsch, V., Rüterjans, H., Glaubitz, C., and Bernhard, F. (2004) High level cell-free expression and specific labeling of integral membrane proteins, *Eur. J. Biochem. 271*, 568−580.

BI050676C